Turkish Journal of Electrical Engineering & Computer Sciences

http://journals.tubitak.gov.tr/elektrik/

Research Article

Turk J Elec Eng & Comp Sci
(2020) 28: 2375 – 2384

doi:10.3906/elk-2005-39

Fiber optic chemical sensors for water testing by using fiber loop ringdown spectroscopy technique

Malik KAYA*
Eskişehir Osmangazi University, Vocational School of Health Service, Eskişehir, Turkey

Received: 05.05.2020 • **Accepted/Published Online:** 10.08.2020 • **Final Version:** 25.09.2020

Abstract: Real-time response, low cost, sensitive and easy setup fiber optic chemical sensors were fabricated by etching a part of single mode fiber in hydrofluoric (HF) acid solution and tested in different water samples such as tap water, DI water, salty and sugar water with different concentrations to record ringdown time (RDT) differences between media due to refractive index differences by employing the fiber loop ringdown (FLRD) spectroscopy technique. Baseline stability of 0.63% and the minimum detectable RDT of 5.05 μs for this kind of fiber optic chemical sensors were obtained. Fabricated sensors were coated with N,N-Diethyl-p-phenylenediamine for the first time and tested in several water solutions. Afterwards, the sensors were immersed into salty and sugar water solutions in different concentrations. The results showed that this kind of FLRDS fiber optic chemical sensors can be applicable to trace chemicals in water solutions. Moreover, fiber optic sensors can be specially modified to trace specifically any target chemicals in solutions for the special purpose and the early detection.

Key words: Fiber optic sensors, chemical trace, fiber optic, fiber optic chemical sensors, evanescent field, FLRD spectroscopy technique

1. Introduction

Fiber optic sensors have inspired researchers for a long time for their widespread application area because of high advantages such as light weight, long distance applications, low data loss, small size, high sensitivity and immunity to electromagnetic interferences. The fiber loop ringdown spectroscopy (FLRDS) technique offers multifunctionality in measurements because its working principle is based on the cavity ringdown spectroscopy (CRDS) technique. Since a space between high reflective mirrors is used as the cavity in CRDS technique, a fiber loop in several lengths is employed as the cavity in the FLRDS technique. Since having time domain technique characteristics, in FLRDS, a small part of a laser beam is coupled into the fiber loop for several interactions with measurands, hence the measurement stability and sensitivity dramatically increase. The FLRDS technique has been utilized to measure various parameters such as refractive index [1–3], pressure [4–6], strain [7–9], magnetic field [10], temperature [11, 12], biological species [13–15], and chemicals [16–18]. Chemical trace detection in both gaseous and liquid media is highly important due to measuring hazardous and excessive chemicals such as chlorine [19], ammonia [20], acetone [3], methane [21], carbon monoxide [22] and phosphate [23]. For chemical trace detection, Nguyen et al. fabricated a fiber optic chloride sensor by employing fluorescence quenching of acridinium dye so that the dye bounds covalently to chloride ions [24]. They obtained sensitivity for chloride sensor at larger concentrations than 0.1 M. In the other study, Ding et al. developed fiber optic sensor based on

*Correspondence: malikkaya@ogu.edu.tr

suspended core fiber optic to trace chloride in concrete by immobilizing lucigenin on the inner surface of the fiber with dip coating technique [25]. Choudhury and Yoshino [19] studied detection of chlorine content in drinking water by fiber optic evanescent field (EF) absorption sensor. They used multimode fiber to setup U-shaped sensor probes. In their work, bending radius is critically important for the system sensitivity. They used green LED as light source to detect chlorine. As a sensing element, U-shaped probe with a single fiber is tested in water solutions with different chlorine concentrations. In other work, Yolalmaz et al. [3] studied on detection of chemicals by employing EF-FLRD technique in their system with a light source of 800 nm central wavelength. They tested the sensors in eight different chemicals such as acetone, ethanol, decane, toluene, n-octane, DI water, cyclohexane and dodecane and recorded RDTs by using the refractive index difference of the chemicals with highly sensitive FLRDS system. All aforementioned studies have differences in system setup, laser light source and its central wavelength and used fiber type when compared with our FLRDS system in this work. In this study, a basic design, a simple standalone setup and low-cost fiber optic sensor system by using a CW-FLRDS technique for trace chemicals was introduced. The CW-FLRDS system consists of basic components such as a continuous wave laser diode and its driver, a single mode fiber loop, a free space photodetector, a function generator and an oscilloscope. The aim in this study is to present the trace detection of chemicals in different water solutions with an etched fiber. To the best of my knowledge, the first time the sensor head of this kind of FLRDS chemical sensors coated with N,N-Diethyl-p-phenylenediamine (NDPD) for the purpose of chemical trace testing in several water solutions by utilizing FLRDS technique. Obtained detection limit is independent on any constraint of optical instruments such as oscilloscope and laser. The CW-FLRDS system does not require an optical spectrum analyzer (OSA), additional components such as FPI/FBG or high precise working and extra care to create air-gap/air-cavity to obtain trace chemicals of elements/compounds. The experimental results show that this kind of FLRDS chemical sensors can be applicable to distinguish different solutions and target measurand sensing with special treatment of sensor head and has a high potential to apply for the early detection in broad application field such as land sliding, erosion, structural health monitoring, biomedical applications, crack detection, etc. with additional specific treatment on the sensor head and enhanced system features.

2. Experimental setup

2.1. CW-FLRDS system

Figure 1 presents the laboratory setup of CW-FLRDS system which is consisted of two main parts: the control system and the sensor unit. The control system includes a fiber coupled continuous wave (CW) diode laser (Thorlabs, SFL1550S) and its compact driver (Thorlabs, CLD1015), a free space photodetector (Thorlabs, DET08C/M) and electronic devices for controlling the system. The FLRDS sensor unit composed of a 110 m single mode fiber loop (SMF28e, Corning Inc., Corning, NY, USA) of two identical couplers with a split ratio 99.9:0.1 (Opneti Communication Co., Shenzhen, China) and the fabricated sensor head by chemically etching a part of the fiber loop. The etched fiber length to fabricate sensorhead is 12 cm. The minimum fiber loop length required in the system can be calculated by considering laser source pulse producing time. The fiber loop length must be long enough to allow laser pulse to complete single turn in the loop. Otherwise, seried pulses will interfere and no ringdown will be obtained.

Bare SMF core and cladding diameters are approximately 8.2 μm and 125 μm, respectively. The total optical loss, considering insertion losses, absorption loss and the losses in the couplers, when the laser beam travels through the fiber loop was calculated to be less than 0.40 dB since the fiber splice loss was up to 0.02 dB.

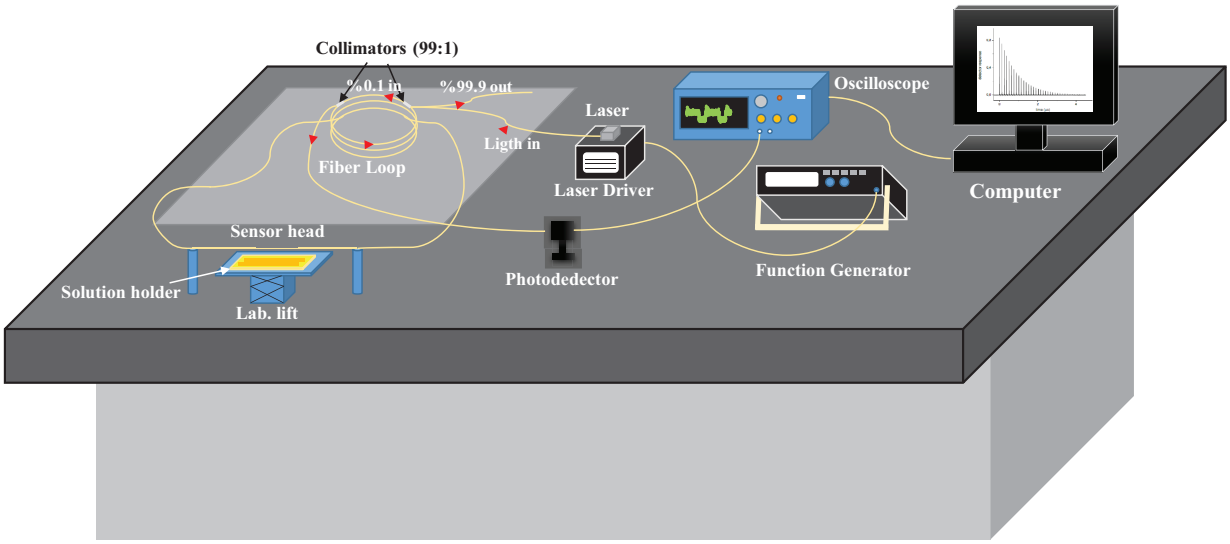

Figure 1. Schematic illustration of the CW-FLRDS system setup.

The laser beam for the system is generated by a 14-pin butterfly external cavity laser diode at central wavelength of 1550 ± 0.5 nm. The laser diode with 40 mW output power is performed at 300 mA operating current and 25 °C operation temperature. The compact driver of laser diode allows to run laser diode at constant temperature and constant current. Generated laser beam was square modulated by the function generator. Only 0.1% of the sent laser beam was injected into the fiber loop by first 99.9:0.1 coupler and the remaining amount separated by the coupler (99.9% portion) so that it can be used as a light source for a new sensor setup. While the small amount of coupled laser beam travels through the fiber loop, 0.1% of it is sent to the photodetector at each round trip by the other 99.9:0.1 coupler. Collected signals by the photodetector were plotted by an oscilloscope (Tektronix TBS1202B, Tektronix, Inc., Beaverton, OR, USA). Plastic jacket of a small part of fiber from the fiber loop was removed and chemically etched during 75 ± 5 min in 48% HF acid solution. The optical loss of the system was increased since the cladding diameter was decreased by etching process, resulting an increase in evanescent field on the sensor head. The optical loss is reciprocal to the cladding diameter and the RDT. As the sensitivity of the sensors increases with radius of the etched sensorhead, a study was carried out on the optimization between sensitivity versus etched radius and optical loss [26]. Figure 2 illustrates a sensor head microscope image before and after etching. During etching process, data were recorded with 5 min steps. The change of the optical loss through etching process was calculated by considering initial and final RDTs of the system as765.44 μs and 733.85 μs, respectively and obtained as 30.29 μdB. Figure 2a shows plastic jacket removed and nonremoved parts of the sensor head. Fiber radii with and without plastic jacket are measured as 245 μm and 125 μm, respectively. In Figure 2b, etched sensor head with the radius of 38 ± 1.5 μm is shown. Figure 2c presents the other part of fabricated sensor head. Afterwards, sensor head was treated with hydrogen peroxide during 30 s and exposed to N,N-Diethyl-p-phenylenediamine (NDPD) solution for 30 s to complete coating process. Choosing NDPD reason is that it can react with chlorine to form azo compound [19] on the sensor head and hence, the detection of chemical trace respect to formed azo compound on the sensor head due to the chlorine reaction ratio can be analyzed. When NDPD is oxidized by chlorine, magenta (red) color is created [19]. While NDPD is oxidized by iron and cupper, it gives blue-colored product [27]. Studies showed that to increase oxidizing ratio of agents and color development by Fe and Cu agents, pH level of the

solution was changed [27, 28]. But for chlorine oxidizing, there is no additional treatment such as changing pH, additional buffer solution etc. In this study, it is assumed that oxidizing with NDPD layer on the sensorhead was mostly created by chlorine.

Figure 2. Image of a fabricated sensor head by chemical etching process under microscope. a) fiber with/without plastic jacket, b) etched fiber and c) another part of etched fiber.

2.2. Working principle

Injected light beam travels many round trips in the fiber loop until it decays. Light beam intensity reduces after every single round trip due to the optical loss and hence, the photodetector receives signals with different intensity at each round. Intensity of received signals I by the photodetector is given by [29, 30]

$$I = I_0 e^{-(Act/nL)} \tag{1}$$

where I_0 is incident beam intensity, A is total fiber transmission loss of the beam per round trip, c is the speed of light, n is the average refractive index and L is the total length of the fiber loop. The time takes to decrease from I to I_0/e is referred as ringdown time (RDT), τ_0, and is written by Eq. (2).

$$\tau_0 = \frac{nL}{cA} \tag{2}$$

$$\tau = \frac{nL}{c(A+B)} \tag{3}$$

For an FLRDS sensor, the total transmission loss does not change because it is calculated by the fiber loop parameters such as insertion losses in the couplers, fiber absorption loss and transmission loss. Once a sensing action is generated on the sensor head such as changing medium around the sensor head, an extra optical loss, B, is created. Changed RDT, τ, due to generated additional optical loss is given by Eq. (3). From Eqs. (2) and (3), additional optical loss B is obtained to be

$$B = \frac{nL}{c}\left(\frac{1}{\tau} - \frac{1}{\tau_0}\right) \tag{4}$$

By using Eq. (4), when a sensing action such as strain, pressure or medium around the sensor head is applied on the sensor head, it can be identified by obtaining RDTs with and without the sensing action. For this kind of FLRDS chemical sensors, B denotes the optical loss differences between air and water solutions. Since

water and air has different refractive indexes, optical refractive index of the sensor head and water interface is affected whenever the sensor head immersed into the water solution. The amount of evanescent field (EF) scattering loss changes with changing refractive index and hence recorded RDTs between air and water are different [31–33]. The minimum measurable optical loss can be obtained by

$$B_{min} = (\frac{t_r}{\tau_0})(\frac{\sigma}{\tau_{ave}}) = (\frac{1}{m})(\frac{\sigma}{\tau_{ave}}) \tag{5}$$

where t_r is the round trip time of the laser beam in the loop, m is the number of rounds, and σ is the standard deviation. σ/τ_{ave} is the stability of baseline. The minimum detectable optical loss of the system is calculated by using Eq.5 as 31.5 μdB. The minimum measurable RDT, τ_{min} is obtained as 5.05 μs by the baseline stability and sensor RDT without any action on the sensor head. In this work, t_r is calculated as 538.7 ns for 110 m loop and m is obtained as 20. Further details on baseline stability calculations can be found in references [30, 32, 33].

3. Results and discussion

Figure 3 shows the baseline stability of the NDPD coated FLRDS chemical sensor. Each data point in the graph is the average of at least five data collected at every 10 s. The baseline stability was calculated by considering collected RDT data when the sensor head is in air and no any additional loss created on the sensor. The average RDT was obtained as 800.85 μs and the standard deviation of the data was calculated as 5.076 s. Based on the obtained baseline stability of 0.63%, the minimum detectable RDT of the FLRDS chemical sensor is calculated as 5.05 μs so that it is the limit for the sensor system in which two different media can be differentiated. The optical loss of the system is the critical parameter to compare differences of the media, but in this study, even though the minimum detectable RDT is used for the comparisons, the optical loss was considered and calculated at each step. In all data graphics, while y-axes show the RDT values, x-axes present time. Each data point in the graphics is averaged of several collected data at every 10 s.

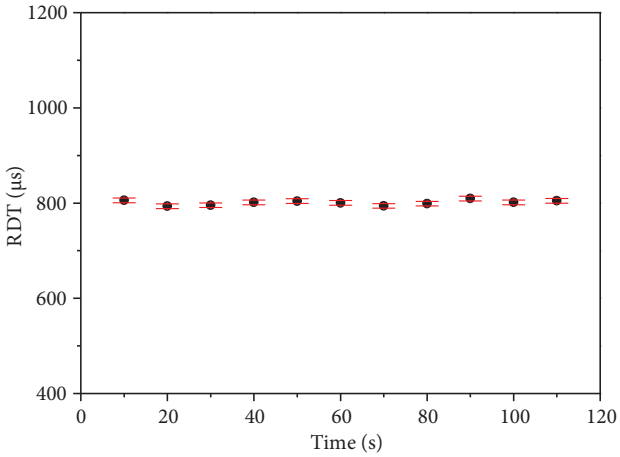

Figure 3. Baseline stability of the FLRDS chemical sensor with 10 cm sensor head.

Figure 4 shows two sets of data collected from tap water and DI water solutions. The NDPD coated sensor was first exposed to air and then immersed into the water solutions. The processes (air-water tests) were repeated to present the repeatability of the sensors. Created optical loss between air-tap water when the

sensorhead is immersed into tap water from air is calculated by using Eq. 4 as 75 μdB. The minimum detectable optical loss of the system is calculated by Eq. 5 as 31.5 μdB. Therefore, these two media can be differentiated by this kind of sensors. As mentioned before, the comparisons will be carried on by using minimum RDTs. When the sensor head was in air, recorded RDT was 800.33 μs. As soon as the sensorhead was immersed into tap water solution, RDT was increased to 900.86 μs. Difference between first air-tap water data in Figure 4a is 100.01 μs which is higher than the minimum measurable RDT of the sensor system. Therefore, this difference between two media can be obtainable by this kind of chemical sensors. Similarly, recorded RDT was 803.51 μs when the sensorhead was in air and the RDT was increased to 924.52 μs when the sensorhead was immersed into the solution. The RDT difference between first adjacent data in Figure 4b (air-DI water) is calculated as 111.01 μs which is also higher than the minimum measurable RDT so that it can be measurable.

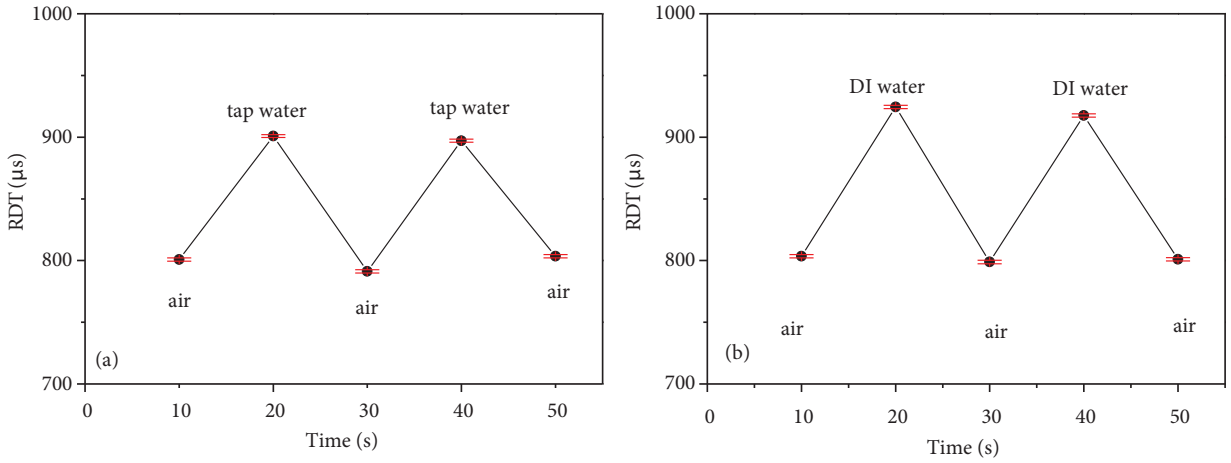

Figure 4. RDT measurements of fiber optic chemical sensors in a) tap water and b) DI water solutions.

Figure 5 presents the test of an NDPD coated FLRDS chemical sensor in different salty water concentrations. The sensor head was first immersed into DI water solution to show reproducibility and repeatability of the sensor. First RDTs in air and DI water solution were recorded as 800.87 μs and 925.77 μs, respectively. Next, the sensor head was immersed into 0.1 M salty water solution and the RDT was recorded 875.83 μs. Since the refractive indexes between tap water and 0.1 M salty water are different, recorded RDTs when the sensorhead immersed into solutions are different due to the difference in created optical loss. The evanecsent field penetration around the sensorhead in each solution/media changes related to the solution/media refractive index. Therefore, the system optical loss changes respect to sensorhead's exposed media. After the sensor head rinsed with DI water, it was immersed into 0.05 M salty water solution. The RDT was recorded as 907.36 μs. RDT differences both between 0.05 M and 0.1 M salty water solutions and 0.05 M salty water and DI water solutions are 8.10 μs and 12.94 μs, respectively that both of them are higher than the minimum measurable RDT. Therefore, these media can also be distinguishable by the sensor. RDT values when the sensor head was in DI water were almost repeatable as well as RDT values when the sensor head was exposed to air after testing in each solution. Recorded RDTs show that this kind of FLRDS chemical sensors can be employed to distinguish different solutions. Each data point in Figure 5 was obtained by taking the average of at least three data.

Figure 6 shows the data set of FLRDS chemical sensor in sugar water with different concentrations. Following the same steps as in Figure 5, the FLRDS chemical sensor was immersed into DI water solution

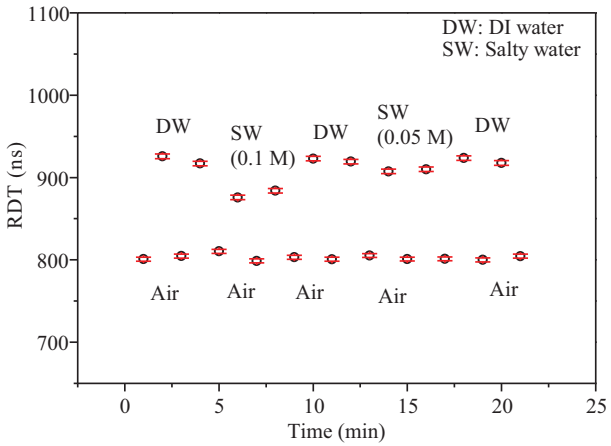

Figure 5. FLRDS chemical sensor data set collected from different salty water concentrations.

twice to show sensor reproducibility and repeatability. First RDTs in air and DI water solution were recorded as 789.33 μs and 902.07 μs, respectively. After DI water solution, the sensor was immersed into 0.1 M sugar solution and the RDT was recorded as 935.12 μs. After rinsed in DI water, the sensor was immersed into 0.05 M sugar solution. The RDT was obtained as 915.13 μs. RDT differences between 0.1 M and 0.05 M sugar water solutions and 0.05 M sugar water and DI water solutions are obtained as 6.69 μs and 150.75 μs, respectively. Because all solutions had different refracitve indexes, the FLRDS system optical loss changed when the sensorhead immersed into the solutions, and hence, different RDT values can be recorded. Because these obtained differences are higher than the minimum detectable RDT of the sensor system, these different media can also be detectable by this kind of FLRDS chemical sensors. All recorded RDTs show that the FLRDS chemical sensors can be utilized for trace chemical sensing in sugar water solution as well.

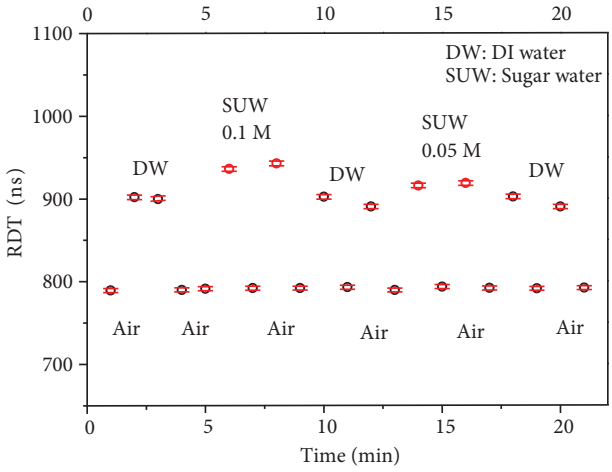

Figure 6. FLRDS chemical sensor data set collected from different sugar water concentrations.

In this study, FLRDS chemical sensors were created by etching a part of SMF in 110 m fiber loop and tested in several water solutions such as tap water, DI water, salty water and sugar water with different concentrations. As mentioned in Ref. [19], NDPD reacts with chlorine and create azo compound. In our

study, NDPD coated fiber optic sensors were tested in tap water and salty water solutions. From the obtained results, two possibilities can be asserted: i) NDPD coating does not have any impact on the sensor sensitivity because the measured RDT after the sensor head exposed from tap water or any other salty water solutions did not change critically. ii) Azo compounds were formed on the sensor head, but our FLRDS system is not so sensitive that we can determine the change. To observe the difference, system baseline must be more stable and the minimum detectable RDT should be lower than the measurable value. Better baseline stability and lower detectable RDT in an FLRD system can be obtained by using a narrow bandwidth laser, a photodetector having a narrower operation wavelength, lower intrinsic loss in the FLRDS sensor system setup, etc. [3, 34]. Gangopadhyay et al developed a chemical sensor with 4 m SMF fiber loop by using 2.53 mm etched sensor head for detection of different chemicals such dimethyl sulfoxide, ethilenediamine, and ethanol [16]. They were built fiber loop with three different splitting ratio of 99:1, 96.5:3.5 and 99.5:0.5. System sensitivity may be limited by higher splitting ratio and lower sensor head when compared with our system. In our study, NDPD coating did not have significant effect on the sensor sensitivity to observe the difference. Fabricated FLRDS chemical sensors were tested in various water solutions such as tap water, DI water, salty and sugar water with different concentrations. The results indicate that this kind of FLRDS chemical sensors can be employed for trace chemical detection in liquids. Furthermore, enhanced baseline and sensitivity will yield FLRDS sensors to be applied for early detection.

4. Conclusion

In this study, a standalone, simple, sensitive, and low-cost fiber optic sensor system setup by using a CW-FLRDS technique for chemical trace measurement was presented. The CW-FLRDS system composed of only main components such as a continuous wave laser diode with its driver, a 110 m single mode fiber loop, a free space photodetector, a function generator and an oscilloscope. FLRDS chemical sensors have the baseline stability of 0.63% and the minimum detectable RDT of 5.05 μs. Fabricated FLRDS chemical sensors were coated with NDPD for the purpose of selectivity of chlorine chemical so that NDPD coating has no crucial impact on the sensor sensitivity. Several water solutions such as tap water, DI water, salty and sugar water with different concentrations were tested in this study with FLRDS chemical sensors and obtained results indicate that this kind of FLRDS chemical sensors can differentiate solutions. For the target sensing with higher sensitivity and to be applied fort the early detection purpose, the chemical sensors should be selectively coated with materials which is sensitive to the selected measurands and the system components such as laser source, photodetector, total loss of the fiber loop, etc. must be enhanced.

Acknowledgment

This work was partially supported by ESOGU BAP with the project code 2019-2001. Microscope images were taken in Laser Spectroscopy Laboratory at Chemistry Department, METU (Ankara, Turkey). Author also thanks to Prof. Dr. Okan Esentürk in Chemistry Department, METU for his valuable support and gives opportunity to use Laser Spectroscopy Laboratory.

References

[1] Ni N, Chan CC, Xia L, Shum P. Fiber cavity ring-down refractive index sensor. IEEE Photonics Technology Letters 2008; 20: 1351-1353. doi: 10.1109/LPT.2008.926866

[2] Wang C, Herath C. High-sensitivity fiber-loop ringdown refractive index sensors using single-mode fiber. Optics Letters 2010; 35: 1629-1631. doi: 10.1364/OL.35.001629

[3] Yolalmaz A, Danışman MF, Esenturk O. Discrimination of chemicals via refractive index by EF-FLRD. Applied Physics B 2019; 125: 156-165. doi: 10.1007/s00340-019-7261-5

[4] Wang C, Scherrer S. Fiber ringdown pressure sensors. Optics Letters 2004; 29: 352-354. doi: 10.1364/OL.29.000352

[5] Wang C, Scherrer S. Fiber loop ringdown for physical sensors development: Pressure sensor. Applied Optics 2005; 43: 6458-6464. doi: 10.1364/AO.43.006458

[6] Qiu H, Qiu Y, Chen Z, Fu B, Chen X et al. Multimode fiber ring-down pressure sensor. Microwave Optical Technology Letters 2007; 49: 1698-1700. doi: 10.1002/mop.22553

[7] Zhou W, Wong WC, Chan CC, Shao LY, Dong X. Highly sensitive fiber loop ringdown strain sensor using photonic crystal fiber interferometer. Applied Optics 2011; 50: 3087-3092. doi: 10.1364/AO.50.003087

[8] Ghimire M, Wang C. Highly sensitive fiber loop ringdown strain sensor with low temperature sensitivity. Measurement Science Technology 2017; 28: 105101/1-10. doi: 10.1088/1361-6501/aa82a3

[9] Kaya M, Esenturk O. Study of strain measurement by fiber optic sensors with a sensitive fiber loop ringdown spectrometer. Optical Fiber Technology 2020; 54: 102070/1-7. doi: 10.1016/j.yofte.2019.102070

[10] Sun B, Shen T, Feng T. Fiber-loop ring-down magnetic field and temperature sensing. Optik 2017; 147: 170-179. doi: 10.1016/j.ijleo.2017.08.093

[11] Wang C. Fiber ringdown temperature sensors. Optical Engineering 2005; 44: 030503/1-3. doi: 10.1117/1.1869512

[12] Qin C, Yang L, Yang J, Tian J, Wang J et al. Temperature sensing based on chaotic correlation fiber loop ring down system. Optical Fiber Technology 2019; 47: 141-146. doi: 10.1016/j.yofte.2018.11.027

[13] Herath C, Wang C, Kaya M, Chevalier D. Fiber loop ringdown DNA and bacteria sensors. Journal of Biomedical Optics 2011; 16: 050501. doi: 10.1117/1.3572046

[14] Wang C, Kaya M, Wang C. Evanescent field-fiber loop ringdown glucose sensor. Journal of Biomedical Optics 2012; 17: 037004. doi: 10.1117/1.JBO.17.3.037004

[15] Kaya M, Wang C. Fiber loop ringdown glucose sensors: initial tests in human diabetic urines. Fiber Optic Sensors and Applications XI 2014; 9098: 90980O. doi: 10.1117/12.2049929

[16] Gangopadhyay TK, Giorgini A, Halder A, Pal M, Paul MC et al. Detection of chemicals using a novel fiber-optic sensor element built in fiber loop ring-resonators. Sensors and Actuators B: Chemical 2015; 206: 327-335. doi: 10.1016/j.snb.2014.09.024

[17] Yolalmaz A, Sadroud FH, Danışman MF, Esenturk O. Intracavity gas detection with fiber loop ring down spectroscopy. Optics Communications 2017; 396: 141-145. doi: 10.1016/j.optcom.2017.03.045

[18] Kaya M, Wang C. Detection of trace elements in DI water and comparison of several water solutions by using EF-FLRD chemical sensors. AIP Conference Proceedings 2017; 1809: 020027. doi: 10.1063/1.4975442

[19] Choudhury PK, Yoshino T. On the fiber-optic chlorine sensor with enhanced sensitivity based on the study of evanescent field absorption spectroscopy. Optik 2004; 115: 329-333. doi: 10.1078/0030-4026-00375

[20] Cao W, Duan Y. Optical fiber-based evanescent ammonia sensor. Sensors and Actuators B: Chemical 2005; 110: 252-259. doi: 10.1016/j.snb.2005.02.015

[21] Li M, Dubaniewicz T, Dougherty H, Addis J. Evaluation of fiber optic methane sensor using a smoke chamber. International Journal of Mining Science and Technology 2018; 28: 969-974. doi: 10.1016/j.ijmst.2018.05.010

[22] Zhu S, Chen Y, Gang Z, Sa J. A near-infrared optical fiber sensor for carbon monoxide concentration monitoring. Microwave Optic Technology Letters 2010; 52: 2192-2195. doi: 10.1002/mop.25469

[23] Varghese BP, Pillai AAB, Naduvil MK. Fiber optic sensor for the detection of ammonia, phosphate and iron in water. Journal of Optics 2013; 42: 78-82. doi: 10.1007/s12596-013-0121-5

[24] Nguyen TH, Lin YC, Chen CT, Surre F, Venugopalan T et al. Fibre optic chloride sensor based on fluorescence quenching of an acridinium dye. Proceedings of SPIE 2009; 7503: 750314/1-5. doi: 10.1117/12.835607

[25] Ding L, Li Z, Ding Q, Shen X, Yuan Y et al. Microstructured optical fiber based chloride ion sensing method for concrete health monitoring. Sensors and Actuators B: Chemical 2018; 260: 763-769. doi: 10.1016/j.snb.2018.01.091

[26] Yolalmaz A. Utilization of fiber loop ring down technique for sensing applications. MSc, Middle East Technical University, Ankara, Turkey, 2017.

[27] Lunvongsa ST, Takayanagi M, Oshima S, Motomizu S. Novel catalytic oxidative coupling reaction of N,N-dimethyl-p-phenylenediamine with 1,3-phenylenediamine and its applications to the determination of copper and iron at trace levels by flow injection technique. Analytica Chimica Acta 2006; 576 (2006): 261-269.

[28] Hirayama K, Unohara N. Spectrophotometric catalytic determination of an ultratrace amount of iron(III) in water based on the oxidation of /V ,/V-dimethyl-p -phenylenediamine by hydrogen peroxide. Analytical Chemistry 1988; 60: 2573-2577.

[29] Sahay P, Kaya M, Wang C. Fiber loop ringdown sensor for potential real-time monitoring of cracks in concrete structures: an exploratory study. Sensors 2013; 13: 39-57. doi: 10.3390/s130100039

[30] Kaya M, Sahay P, Wang C. Reproducibly reversible fiber loop ringdown water sensor embedded in concrete and grout for water monitoring. Sensors and Actuators B: Chemical 2013; 176: 803-810. doi: 10.1016/j.snb.2012.10.036

[31] Wang C, Herath C. Fabrication and characterization of fiber loop ringdown evanescent field sensors. Measurement Science and Technology 2010; 21 (8): 085205/1-085205/10.

[32] Cengiz B. Fiber loop ring down spectroscopy for trace chemical detection. MSc, Middle East Technical University, Ankara, Turkey, 2013.

[33] Kaya M. Time-domain fiber loop ringdown sensor and sensor network. PhD, Mississippi State University, Starkville, MS, USA, 2013.

[34] Liu G, Wu Y, Li K, Hao P, Zhang P et al. Mie scattering-enhanced fiber-optic refractometer. IEEE Photonic Technology Letters 2012; 24: 658-660. doi: 10.1109/LPT.2012.2185786